Journal Pre-proofs

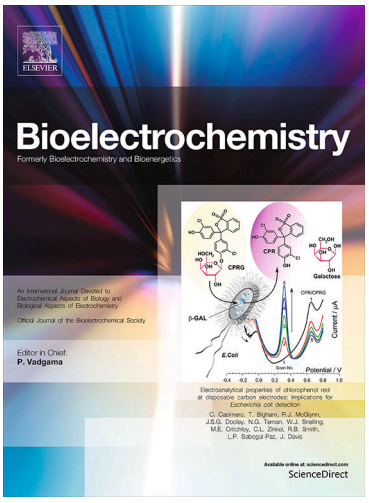

Optimized PAH/Folic acid layer-by-layer films as an electrochemical biosensor for the detection of folate receptors

Abilene Rodrigues Correia, Isabella Sampaio, Edson José Comparetti, Nirton C.S.Vieira, Valtencir Zucolotto

PII: S1567-5394(20)30608-3
DOI: https://doi.org/10.1016/j.bioelechem.2020.107685
Reference: BIOJEC 107685

To appear in: *Bioelectrochemistry*

Received Date: 10 July 2020
Revised Date: 29 September 2020
Accepted Date: 6 October 2020

Please cite this article as: A. Rodrigues Correia, I. Sampaio, E. José Comparetti, N. C.S.Vieira, V. Zucolotto, Optimized PAH/Folic acid layer-by-layer films as an electrochemical biosensor for the detection of folate receptors, *Bioelectrochemistry* (2020), doi: https://doi.org/10.1016/j.bioelechem.2020.107685

Optimized PAH/Folic acid layer-by-layer films as an electrochemical biosensor for the detection of folate receptors

Abilene Rodrigues Correia[1], Isabella Sampaio[1], Edson José Comparetti[1], Nirton C. S.Vieira[1, 2] and Valtencir Zucolotto[1]

[1]GNano – Nanomedicine and Nanotoxicology Group, São Carlos Institute of Physics, University of São Paulo, CP 369, 13560-970, São Carlos, SP, Brazil

[2]Institute of Science and Technology, Federal University of São Paulo, 12231-280, São José dos Campos, SP, Brazil

Corresponding Author: isabellasampaio@ifsc.usp.br

Statistical summary of the article:

Total number of words: 4848

Tables: 1

Figures: 9

Abstract

Folate receptor alpha (FR-α) is a glycoprotein overexpressed in tumor cell surfaces, especially in gynecologic cancers, and can be used as a biomarker for diagnostics. Currently, FRα is quantified by positron emission tomography (PET) or fluorescence imaging techniques. However, these methods are costly and time-consuming. We report on the development of an electrochemical biosensor for FRα detection based on the use of nanostructured layer-by-layer (LbL) films as modified electrodes. Multilayer films were deposited on indium tin oxide (ITO) electrodes by the alternately assembling of positively charged polyallylamine hydrochloride (PAH) and negatively charged folic acid (FA), used as the biorecognition element. UV-vis and FTIR spectroscopies revealed the successful PAH and FA adsorption on ITO. Devices performance was evaluated by cyclic voltammetry (CV) and electrochemical impedance spectroscopy (EIS). The [PAH/FA] films presented a good reproducibility (RSD of 1.12%) and stability when stored in the Tris-HCl solution (RSD 6.7%). The biosensor electrochemical response exhibited a linear relationship with FRα concentration in the range from 10 to 40 nM. The limit of detection reached for CV and EIS measurements were 0.7 and 1.5 nM, respectively. As a proof-of-concept, we show that the devices can differenciate tumor cells from healthy cell, showing an excellent selectivity. The biosensor device based on [PAH/FA] films represents a promising strategy for a simple, rapid, and low-cost cancer diagnosis through FRα quantification on the surface of cancer cells.

Keywords: Folate receptor detection; Layer-by-layer self-assembly; Electrochemical biosensor; Multilayer films; folic acid

1.Introduction

Folate receptor (FR) is a cell membrane glycoprotein with a high binding affinity to folic acid (FA), an essential vitamin, highly consumed by proliferating cells because of its role in the synthesis of nucleotides [1,2]. In healthy tissues, FRα isoform is expressed at low levels, being usually located in the apical membrane, which is inaccessible to blood since it is oriented towards the lumen. However, FRα is overexpressed in the basolateral membrane – oriented away from the lumen - of many epithelial-derived tumors such as ovarian, cervical, prostate, and kidney carcinomas, and their levels may be associated with tumor aggressiveness [3–7]. Therefore, this glycoprotein represents an important biomarker of cancer cells, and can be used to predict the tumor stage [3,8].

The detection of folate receptors is usually performed by fluorescence imaging techniques in which folic acid labeled with a fluorescent probe is used, or by positron emission tomography using radioligands [3,5,9–11]. However, these methods are time-consuming and present disadvantages, such as the use of toxic radioligands and low sensitivity since small dyes, for example, FA-fluorescein isothiocyanate, do not remain in the systemic circulation for a long time, not reaching the tumor efficiently [3,5,9–11]. To overcome these challenges, novel strategies for FR detection and quantification are required.

Electrochemical biosensors have been employed in the medical area for diagnosis of many diseases mainly because they are easy-to-use and can provide rapid response under the point-of-care concept, with high selectivity and sensitivity [12–15]. For folate receptors detection, in particular, Liu et al. reported an electrochemical method to identify FR positive tumor cells. The authors used gold nanoparticles modified with FA, which were complexed to cysteamine molecules and assembled on gold electrodes [16]. Damiati et al. also developed a biosensor for FR detection by using gold electrodes functionalized with bacteria proteins conjugated to FA [8]. However, the methodologies used in these biosensors involve the covalent attachment of FA to pre-covered electrodes, which is a longer process and requires costly reagents. To overcome these challenges, the electrostatic layer-by-layer (LbL) self-assembly technique is very attractive because of its simplicity and low-cost. When used in the immobilization of biomolecules, the LbL technique allows the assembly of nanostructured films within which the conformational structure and the function of the biomolecules are preserved [17–19]. Many studies have

reported LbL-based biosensors for detecting proteins [20], DNA [21], and lipids [17]. It has been demonstrated that even enzymes which are very sensitive to the microenvironment, as uricase [22] and glucose oxidase [23], keep their bioactivity upon immobilization in LbL films.

In this study we developed a novel electrochemical biosensor for the detection of FRα. The biosensor devices were constructed by the alternating assembling of poly allylamine hydrochloride (PAH) as cationic polyelectrolyte and FA as the anionic electrolyte on the surface of indium-tin oxide (ITO) substrates. The [PAH/FA] films were characterized by Ultraviolet-visible (UV-Vis) and Fourier transform infrared spectroscopy (FTIR) spectroscopies and atomic force microscopy (AFM). To enhance biosensors performance, experimental parameters as the number of bilayers, immersing time, and pH of the dispersions were evaluated and optimized. Cyclic voltammetry (CV) and electrochemical impedance spectroscopy (EIS) techniques were used to monitor the binding of FRα to folic acid immobilized onto the ITO surface. The developed biosensors were able to detect FRα at different concentrations with excellent reproducibility and stability, demonstrating the great potential of the LbL films for applications in the rapid, simple, and low-cost FRα detection for future aid in cancer diagnosis upon quantifying the folate receptors present in the patient's cells.

2. Materials and methods

2.1. Materials

ITO substrates with surface resistance of 8-12 Ω were purchased from Delta Technologies (USA). Polyallylamine hydrochloride, bovine serum albumin, folic acid, and folate receptor alpha were acquired from Sigma-Aldrich. Phosphate buffered saline (PBS) at pH 8.0 was prepared using Sigma-Aldrich reagents: potassium phosphate monobasic 14 mM, dibasic sodium phosphate 87 mM, sodium chloride 136.7 M, potassium chloride 2.7 mM. Phosphate buffer (PB) 100 mM pH 8.0 was also prepared with potassium phosphate monobasic 61 mM and dibasic sodium phosphate 38 mM. Tris(hydroxymethyl)aminomethane (Sigma-Aldrich) was used to prepare Tris-HCl buffer 100 mM at pH 8.0. The salts used in KCl 100 mM and $NaNO_3$ 100 mM both at pH 8.0 were acquired from Sigma-Aldrich. Electrochemical measurements were performed using 1 mM potassium ferricyanide/potassium ferrocyanide (Sigma-Aldrich) as a redox

couple. For detection tests, solutions with different concentrations of FRα were prepared in Tris-HCl buffer. All aqueous solutions were prepared using Milli-Q purified ultrapure water with 18.2 MΩ.cm resistivity.

2.2 Deposition of $[PAH/FA]_n$ films

ITO substrates were cleaned by subsequent sonication in acetone, isopropanol, and ethanol for 5 min, and ultrapure water for 15 min, using an ultrasonic bath. This procedure was repeated three times. Finally, the electrodes were sonicated in alcoholic KOH solution (1M) for 5 min, rinsed with ultrapure water and dried in N_2 flow. LbL films were assembled onto ITO surface by immersion, firstly in aqueous PAH solution (1mg/mL, pH 6.0) for 3 min and then in ultrapure water (pH 6.0) to remove the cationic polymer excess. The bilayer assembling was completed by immersing the ITO electrode in FA solution (1mg/mL, pH 8.0) with subsequent removal of the FA excess in ultrapure water (pH 8.0). This process was repeated to obtain the desired number of bilayers for each analysis. Fig. 1 shows the schematic representation of the LbL process.

2.3 Cell culture

Cervical cancer cells (HeLa) and Human Mammary Epithelial Cells (HMEC) were cultured in the complete medium [Eagle's medium and MCDB 131 medium, respectively, supplemented with 10% fetal bovine serum (FBS), 1% sodium pyruvate, 1% non-essential amino acids, 1% antibiotic and antimycotic (Life Technologies), and HEPES (Sigma)] at 37 °C under 5% of CO_2. The cells were trypsinized with 0.05% trypsin-EDTA (Gibco) to release them from the bottom of the bottle and separated from the medium by centrifugation at 1200 rpm for 4 min followed by washing twice with PBS. To prepare the cell suspensions for the detection assays, the cells were re-dispersed in 1 ml of PBS and diluted to the concentration of 10^6 cells/mL.

2.3 Characterization of LbL films

UV-Vis spectroscopy was employed to monitor the multilayers formation on quartz substrates (area = 450 mm^2). The absorption spectra were collected using a U-2900 spectrophotometer (Hitachi, Japan). AFM images were obtained using a NanoSurf Flexa microscope (Nanosurf, Switzerland) in tapping mode with a resonant frequency of 300 kHz and spring constant k = 40 N/m. Gwyddion software was used to analyze the images

and to determine the average roughness of the LbL films. FTIR spectra of pure FA, PAH, and $[PAH/FA]_{40}$ were measured using a Nicolet iS50 FTIR spectrometer (Thermo scientific, EUA).

2.4 Electrochemical measurements

The experiments were performed in a three-electrode electrochemical cell: modified ITO substrates (area = 50 mm^2) as working electrode, platinum plate (area = 50 mm^2) as counter-electrode and Ag/AgCl electrode (KCl 3.0 M) as reference. Electrochemical measurements were carried out using a potentiostat/galvanostat PGSTAT30 (Metrohm Autolab) and 100 mM $NaNO_3$ as supporting electrolyte containing 1 mM $[Fe(CN)_6]^{3-/4-}$ as the redox probe. CV measurements were performed in the potential range from -0.6 to 1.1 V and at a 100 mV/s scan rate. For EIS analyses, 10 mV AC perturbation at open circuit potential was applied, and the impedance was measured in frequencies from 10 kHz to 0.1 Hz. FRA (Frequency Response Analyzer) software (Autolab) was used to fit the equivalent circuit model and determine the charge transfer resistance (R_{CT}).

3. Results and discussion

3.1 Characterization of $[PAH/FA]_n$ LbL films

The $[PAH/FA]_n$ films morphology was investigated by AFM analyses using a Si/SiO_2 substrate covered with 20 bilayers of PAH/FA. The AFM images shown in Fig. 2 reveals a fully packed island structures on the film surface with an average roughness of 17 nm. This morphological profile is very desirable for electrochemical biosensors because rough electrodes present high electroactive areas that improve sensitivity by increasing the number of active sites capable of biding biorecognition molecules [24,25].

Fig. 3 shows the FTIR spectra of FA, PAH, and $[PAH/FA]_{40}$. FTIR spectrum of pure FA exhibits the characteristic bands at 1510 and 3327 cm^{-1} attributed to pterin ring, at 1607 cm^{-1} assigned to N-H bending vibration mode, and the stretching vibration of C=O at 1696 cm^{-1} [26]. Bands at 1191 and 1450 cm^{-1} related to C-H bending vibrations of p-aminobenzoic acid moiety are also observed [27]. PAH spectrum presented bands at 1605 and 1519 cm^{-1} attributed to N-H angular deformation and at 2923 cm^{-1} assigned to C-H stretching[28–30]. PAH and FA characteristic bands were observed in the

$[PAH/FA]_{40}$ film spectrum. Moreover, the spectrum of the LbL film presented a small shift in three bands concerning to pure FA, from 1191, 1450, and 1696 cm^{-1} to 1190, 1453, and 1693 cm^{-1}, indicating the interaction between FA and PAH molecules.

3.2 Optimization of $[PAH/FA]_n$ LbL films assembly

The LbL self-assembly procedure was performed using FA solutions at pH 8.0, 10.0, and 12.0 to investigate the pH influence on the growth of [PAH/FA] LbL films. These pH values were established because for pH above 8.0, the FA molecule is negatively charged and therefore acts as an anionic electrolyte. The polycationic solution was used at pH 6.0 since PAH exhibits a pKa between 8-9. Fig. 4A shows the spectra of a $[PAH/FA]_{10}$ film using FA solutions at pH 8.0, 10.0, and 12.0. The spectra presented a maximum absorption at 290 nm assigned to $\pi-\pi^*$ electronic transitions from p-aminobenzoic acid moiety of the FA and a broad band around 350 nm related to $n-\pi^*$ transitions in the pterin moiety [27,31,32]. By comparing the films in different pH values, the highest intensity of the bands was obtained for the FA solution with pH 8.0. At pH 10.0 there was a decrease in the absorbance at 290 nm and no significant change in the band around 350 nm. When the pH value was increased to 12.0, a remarkable decrease was observed in the entire spectrum. The absorbance at 290 nm was also analyzed in films assembled with different numbers of bilayers for the three pH values studied. Fig. 4B shows that there is a gradual increase in absorbance as the [PAH/FA] bilayers are added, and a linear behavior was observed for films grown at pH 8.0 and 10.0. For films assembled at pH 12.0, a decrease in absorbance intensity was observed, indicating a possible change in the chemical structure of FA at higher pH values, affecting the binding to folate receptors. Hence, the FA solution at pH 8.0 was selected for the subsequent analyses.

The immersion time required for the adsorption of FA on the LbL films was also optimized. Films containing 1, 2, and 4 PAH/FA bilayers were fabricated by immersing quartz electrodes in the PAH solution for 3 min, with the subsequent FA adsorption being performed at different immersion times. The absorbance at 290 nm was collected for each time studied, as shown in Fig. S1. An increase in absorbance was observed for immersions carried out up to 3 min for the three studied films, followed by an equilibrium state, indicating that for longer periods, there is no additional FA adsorption. FA immersion time was then set as 3 min for the following studies.

ITO electrodes modified with $[PAH/FA]_3$ were stored in PBS, PB, KCl, and Tris-HCl buffers for up to 24 h. At determined intervals, the electrodes were submitted to the electrochemical analyses. The Nyquist plots (Fig. 5) show impedance spectra containing a semicircle in the high-frequency region and a linear part at low frequencies, typical of a Randles equivalent circuit. To determine R_{CT} values, the impedance data were fitted to the Randles model. A significant variation in the measurements performed with the electrodes stored in the PB and PBS solutions was observed, with an increase in R_{CT} values as the storage time was extended. Possibly, such behavior is due to the instability of the FA molecules caused by the phosphate molecules present in the buffers, as previously discussed by Arcot e Shrestha [33]. Films stored in KCl also exhibited an increase in R_{CT} values, but the variations were subtler. In the latter case, Cl^- ions can adsorb on the film surface [34], causing a decrease in charge transfer. Finally, the storage in the Tris-HCl buffer provided stability for the electrodes modified with [PAH/FA] since no significant changes in R_{CT} values were observed. The relative standard deviation (RSD) was calculated at 6.7%. The electrochemical analyses indicated that, among the tested solutions, the Tris-HCl buffer is the most appropriate to store the electrodes.

The influence of the number of PAH/FA bilayers on the electrochemical properties of the electrodes was investigated using CV and EIS. ITO electrodes were subjected to electrochemical measurements and then modified with 1, 3, 5, 7, 9, and 11 PAH/FA bilayers. The change in both anodic peak current (I_{pa}) and R_{CT} parameters after the modification was determined. As shown in Fig 6A, deposition of PAH/FA bilayers caused an increase in the I_{pa}, compared with bare ITO, due to the presence of FA molecules that present amine groups in their protonated form (NH_3^+) at pH 8.0, attracting the electrons from the $[Fe(CN)_6]^{3-/4-}$ redox probe. The variation in I_{pa} ($\Delta I_{pa} = (I_{pa\ modified\ ITO} - I_{pa\ bare\ ITO}) / I_{pa\ bare\ ITO}$) reaches its maximum value (31.2%) for the 5-bilayer PAH/FA electrodes. Additional bilayers deposition resulted in a decrease of I_{pa}, although the variation remained positive (Fig 6B). This behavior is consistent with previous studies and can be attributed to slower electron transfer between the solution and the electrode in thicker LbL films [35,36].

As it can be seen in the Nyquist plots (Fig 6C), the R_{CT} values obtained by EIS measurements were significantly decreased after the assembling of [PAH/FA] film, corroborating the CV results. In this case, the maximum variation in the R_{CT} was found for the electrodes modified with 1 bilayer, which presented a decrease of about 80% (Fig

6D). Comparing the techniques, EIS is more sensitive to chemical changes occurring on the electrode surface. Therefore, aiming at providing a good response for both CV and EIS techniques, the $[PAH/FA]_3$ modified ITO electrodes were chosen for the FR detection tests.

3.3 Folate receptor detection

The electrochemical response of LbL films towards FRα was evaluated using solutions containing the analyte in the concentration range of 10-40 nM. To avoid nonspecific adsorption, $[PAH/FA]_3$ films were previously blocked with BSA solution 1% for 30 min. The electrodes were incubated with the analyte for 30 min, washed with Tris-HCl buffer, and used in the CV and EIS measurements. According to the Nyquist plots shown in Fig. 7A, R_{CT} increases with the FRα concentration, demonstrating the ability of the biosensors to respond to the FRα presence. The analytical curve was obtained from the EIS experiments by plotting ΔR_{CT} versus FRα concentration which demonstrates a linear relationship between these parameters (Fig. 7B). The linear regression analysis showed that the equation better fitted for the relationship was $\Delta R_{CT} = (-20.64 \pm 7.32) + (7.77 \pm 0.36)$ x [FRα] with a correlation coefficient (R^2) of 0.998. Based on the IUPAC model, the limit of detection (LOD) calculated using the standard deviation of three independent electrodes (SD = 3.89) was 1.5 nM.

As observed in the CV measurements, the current in the voltammograms decreased, and the oxidation peak shifted to more positive potentials upon increasing FRα concentration (Fig. 8A). The analytical curve based on the I_{pa} variation was plotted, as shown in Fig. 8B. The equation obtained from linear regression was $\Delta I_{pa} = (2.55 \pm 0.80) + (-0.61 \pm 0.05)$ x [FRα] with correlation coefficient of 0.994. The SD for three independent electrodes in the blank was 0.14 and the LOD calculated was 0.7 nM. The biosensor repeatability was assessed by making 10 successive CV measurements after the interaction with a sample containing 40 nM FRα. The RSD calculated was 3% for Ipa values, showing that good repeatability was achieved by the sensor device. Moreover, the biosensor reproducibility was evaluated using three independent electrodes at the same conditions, and the RSD was calculated at 2.55% for CV and 1.12% for EIS measurements. These values are lower than those presented by other FR biosensors [5,37], demonstrating that the device also presents a high reproducibility. Both techniques were able to detect FRα molecules and exhibited a linear response to the analyte

concentration. For the maximum concentration tested, the $|\Delta R_{CT}|$ and $|\Delta I_{pa}|$ were 279.5% and 19.2%, respectively.

Although several biosensors have been reported to detect folate receptors, many of them are based on more laborious and expensive methodologies. Table 1 summarizes the analytical performance of some of these biosensors and compares them with the device developed in this study The main advantage of the biosensor described here is its simplicity of fabrication and low cost, which make its large scale production and marketing more feasible, in addition to being interesting for application in public health systems. The results show the possibility of using the sensors for folate receptors detection. However, it is important to note that to be applied in the cancer diagnosis, more tests need to be performed using real samples.

3.4 Selectivity test

The selectivity of the LbL-based biosensor was verified by CV and EIS measurements after incubating the modified electrodes for 1 h in suspensions containing healthy cells (HMEC) or tumor cells (HeLa) at a fixed concentration of 10^6 cells/mL. The percentage change in the R_{CT} and I_{pa} parameters was calculated for both cell lines. As shown in Fig. 9, the electrochemical response of the biosensor is much greater for tumor cells in which FRα is overexpressed. The ΔR_{CT} values obtained were 624.4% for tumor cells and 44.9% for healthy cells. The ΔI_{pa} values calculated from the voltammograms were -40% and -4.4% for tumor cells and healthy cells, respectively. These results demonstrate the high selectivity of the biosensor developed in this study and its applicability for cancer detection.

4. Conclusion

We reported the construction of LbL films for electrochemical detection of FRα proteins based on their high affinity to FA molecules. Multilayer films were fabricated on the surface of ITO electrodes by the alternating assembly of positively-charged PAH and negatively-charged FA. The methodology was optimized to improve biosensor performance, and the FRα detection was evaluated in the concentration range of 10-40 nM. Calibration curves were obtained using CV and EIS measurements, which presented a linear response to FRα concentration and LOD of 0.7 and 1.5 nM, respectively. The

selectivity test revealed a huge difference in the electrochemical response of the biosensor to healthy and tumor cells, showing that the biosensor is capable of discriminating the two cell lines tested. Moreover, the biosensor exhibited good reproducibility (RSD of 1.12% for EIS), repeatability, and stability when stored in the Tris-HCl solution. We successfully demonstrated a simple, rapid, and low-cost strategy to the FRα quantification, an important cancer cell biomarker. Therefore, this biosensor represents a promising analytical tool for cancer diagnosis.

Acknowledgments

We gratefully acknowledge to the Conselho Nacional de Desenvolvimento Científico e Tecnológico - CNPq (Grant numbers 158754/2015-8 and 133505/2016-2) and São Paulo Research Foundation - FAPESP (Grant numbers 2018/07508-3 and 18/12670-4) for the financial support and the researchers from Nanomedicine and Nanotoxicology Group for their cooperation in our studies.

References

[1] L. Xu, G. Jiang, H. Chen, Y. Zan, S. Hong, T. Zhang, Y. Zhang, R. Pei, Folic acid-modified fluorescent dye-protein nanoparticles for the targeted tumor cell imaging, Talanta. 194 (2019) 643–648. https://doi.org/10.1016/j.talanta.2018.10.094.

[2] Y. Lu, P.S. Low, F olate-mediated delivery of macromolecular anticancer therapeutic agents, Adv. Drug Deliv. Rev. 54 (2002) 675–693.

[3] S. Dong, J.D.W. Teo, L.Y. Chan, C.L.K. Lee, K. Sou, Far-Red Fluorescent Liposomes for Folate Receptor-targeted Bioimaging, ACS Appl. Nano Mater. 1 (2018) 1009–1013. https://doi.org/10.1021/acsanm.8b00084.

[4] D.J. O'Shannessy, G. Yu, R. Smale, Y.S. Fu, S. Singhal, R.P. Thiel, E.B. Somers, A. Vachani, Folate receptor alpha expression in lung cancer: Diagnostic and prognostic significance, Oncotarget. 3 (2012) 414–425. https://doi.org/10.18632/oncotarget.519.

[5] J. Ni, Q. Wang, W. Yang, M. Zhao, Y. Zhang, L. Guo, B. Qiu, Z. Lin, H.H. Yang, Immobilization free electrochemical biosensor for folate receptor in cancer cells based on terminal protection, Biosens. Bioelectron. 86 (2016) 496–501. https://doi.org/10.1016/j.bios.2016.07.012.

[6] H. Li, Y. Cheng, Y. Liu, B. Chen, Fabrication of folic acid-sensitive gold nanoclusters for turn-on fluorescent imaging of overexpression of folate receptor in tumor

cells, Talanta. 158 (2016) 118–124. https://doi.org/10.1016/j.talanta.2016.05.038.

[7] B. Farran, R.C. Montenegro, P. Kasa, E. Pavitra, Y.S. Huh, Y.K. Han, M.A. Kamal, G.P. Nagaraju, G.S. Rama Raju, Folate-conjugated nanovehicles: Strategies for cancer therapy, Mater. Sci. Eng. C. 107 (2020) 110341. https://doi.org/10.1016/j.msec.2019.110341.

[8] S. Damiati, M. Peacock, R. Mhanna, S. Søpstad, U.B. Sleytr, B. Schuster, Bioinspired detection sensor based on functional nanostructures of S-proteins to target the folate receptors in breast cancer cells, Sensors Actuators, B Chem. 267 (2018) 224–230. https://doi.org/10.1016/j.snb.2018.04.037.

[9] G.M. Van Dam, G. Themelis, L.M.A. Crane, N.J. Harlaar, R.G. Pleijhuis, W. Kelder, A. Sarantopoulos, J.S. De Jong, H.J.G. Arts, A.G.J. Van Der Zee, J. Bart, P.S. Low, V. Ntziachristos, Intraoperative tumor-specific fluorescence imaging in ovarian cancer by folate receptor-α targeting: First in-human results, Nat. Med. 17 (2011) 1315–1319. https://doi.org/10.1038/nm.2472.

[10] Y. Lin, X. Huang, Y. Zhang, D. Chen, J. Wang, F. Luo, L. Guo, B. Qiu, Z. Lin, Electrochemiluminescence Biosensor for the Detection of the Folate Receptor in HeLa Cells Based on Hyperbranched Rolling Circle Amplification and Terminal Protection, ChemElectroChem. 6 (2019) 827–833. https://doi.org/10.1002/celc.201801094.

[11] C.R. Fischer, C. Müller, J. Reber, A. Müller, S.D. Krämer, S.M. Ametamey, R. Schibli, [18F]fluoro-deoxy-glucose folate: A novel PET radiotracer with improved in vivo properties for folate receptor targeting, Bioconjug. Chem. 23 (2012) 805–813. https://doi.org/10.1021/bc200660z.

[12] L.C. Brazaca, I. Sampaio, V. Zucolotto, B.C. Janegitz, Applications of biosensors in Alzheimer's disease diagnosis, Talanta. 210 (2020) 120644. https://doi.org/10.1016/j.talanta.2019.120644.

[13] A. Chamorro-Garcia, A. Merkoçi, Nanobiosensors in diagnostics, Nanobiomedicine. 3 (2016) 1–26. https://doi.org/10.1177/1849543516663574.

[14] M. Manzano, S. Viezzi, S. Mazerat, R.S. Marks, J. Vidic, Rapid and label-free electrochemical DNA biosensor for detecting hepatitis A virus, Biosens. Bioelectron. 100 (2018) 89–95. https://doi.org/10.1016/j.bios.2017.08.043.

[15] H.A.M. Faria, V. Zucolotto, Label-free electrochemical DNA biosensor for zika virus identification, Biosens. Bioelectron. 131 (2019) 149–155. https://doi.org/10.1016/j.bios.2019.02.018.

[16] L. Liu, X. Zhu, D. Zhang, J. Huang, G. Li, An electrochemical method to detect folate receptor positive tumor cells, Electrochem. Commun. 9 (2007) 2547–2550. https://doi.org/10.1016/j.elecom.2007.07.032.

[17] S. Wu, J. Hao, S. Yang, Y. Sun, Y. Wang, W. Zhang, H. Mao, X.M. Song, Layer-by-layer self-assembly film of PEI-reduced graphene oxide composites and cholesterol oxidase for ultrasensitive cholesterol biosensing, Sensors Actuators, B

Chem. 298 (2019) 126856. https://doi.org/10.1016/j.snb.2019.126856.

[18] R.M. Iost, F.N. Crespilho, Layer-by-layer self-assembly and electrochemistry: Applications in biosensing and bioelectronics, Biosens. Bioelectron. 31 (2012) 1–10. https://doi.org/10.1016/j.bios.2011.10.040.

[19] Y. Si, J.W. Park, S. Jung, G.S. Hwang, Y.E. Park, J.E. Lee, H.J. Lee, Voltammetric layer-by-layer biosensor featuring purine nucleoside phosphorylase and chitosan for inosine in human serum solutions, Sensors Actuators, B Chem. 298 (2019) 126840. https://doi.org/10.1016/j.snb.2019.126840.

[20] J. Liu, L. Quan, X. Yu, L. Wang, Quantitative detection of procalcitonin using an electrochemical immunosensor based on MoO3/Au@rGO nanocomposites, Analyst. 144 (2019) 6968–6974. https://doi.org/10.1039/c9an01721f.

[21] M. Rahman, D. Cui, S. Zhou, A. Zhang, D. Chen, A graphene oxide coated gold nanostar based sensing platform for ultrasensitive electrochemical detection of circulating tumor DNA, Anal. Methods. 12 (2020) 440–447. https://doi.org/10.1039/c9ay01620a.

[22] T. Fukuda, H. Muguruma, H. Iwasa, T. Tanaka, A. Hiratsuka, T. Shimizu, K. Tsuji, T. Kishimoto, Electrochemical determination of uric acid in urine and serum with uricase/carbon nanotube /carboxymethylcellulose electrode, Anal. Biochem. 590 (2020) 113533. https://doi.org/10.1016/j.ab.2019.113533.

[23] M. Ferreira, P.A. Fiorito, O.N. Oliveira, S.I. Córdoba De Torresi, Enzyme-mediated amperometric biosensors prepared with the Layer-by-Layer (LbL) adsorption technique, Biosens. Bioelectron. 19 (2004) 1611–1615. https://doi.org/10.1016/j.bios.2003.12.025.

[24] Q. Zhu, B. Liang, Y. Liang, L. Ji, Y. Cai, K. Wu, T. Tu, H. Ren, B. Huang, J. Wei, L. Fang, X. Liang, X. Ye, 3D bimetallic Au/Pt nanoflowers decorated needle-type microelectrode for direct in situ monitoring of ATP secreted from living cells, Biosens. Bioelectron. 153 (2020). https://doi.org/10.1016/j.bios.2020.112019.

[25] S.S. Yoo, S.Y. Kim, K.S. Kim, S. Hong, M.J. Oh, M.G. Nam, W.J. Kim, J. Park, C.H. Chung, W.S. Choe, P.J. Yoo, Controlling inter-sheet-distance in reduced graphene oxide electrodes for highly sensitive electrochemical impedimetric sensing of myoglobin, Sensors Actuators, B Chem. 305 (2020) 127477. https://doi.org/10.1016/j.snb.2019.127477.

[26] Y.Y. He, X.C. Wang, P.K. Jin, B. Zhao, X. Fan, Complexation of anthracene with folic acid studied by FTIR and UV spectroscopies, Spectrochim. Acta - Part A Mol. Biomol. Spectrosc. 72 (2009) 876–879. https://doi.org/10.1016/j.saa.2008.12.021.

[27] M. Baibarac, I. Smaranda, A. Nila, C. Serbschi, Optical properties of folic acid in phosphate buffer solutions: the influence of pH and UV irradiation on the UV-VIS absorption spectra and photoluminescence, Sci. Rep. 9 (2019) 1–11. https://doi.org/10.1038/s41598-019-50721-z.

[28] V. Krishnamurthy, I.L. Kamel, Analysis of Plasma Polymerization of Allylamine by

FTIR, J. Polym. Sci. Part A Polym. Chem. 27 (1989) 1211–1224.

[29] C. Chung, M. Lee, E. Kyung, Characterization of cotton fabric scouring by FT-IR ATR spectroscopy, Carbohydr. Polym. 58 (2004) 417–420. https://doi.org/10.1016/j.carbpol.2004.08.005.

[30] J.J.M.; Cornejo, E. Matsuoka, H. Daiguji, Size control of hollow poly-allylamine hydrochloride / poly-sodium styrene sulfonate microcapsules using the bubble template method, Soft Matter View. 7 (2011) 1897–1902. https://doi.org/10.1039/c0sm00867b.

[31] G. Li, D. Magana, R.B. Dyer, Photoinduced electron transfer in folic acid investigated by ultrafast infrared spectroscopy, J. Phys. Chem. B. 116 (2012) 3467–3475. https://doi.org/10.1021/jp300392a.

[32] P. Chakraborty, P. Bairi, B. Roy, A.K. Nandi, Improved mechanical and electronic properties of Co-assembled folic acid gel with aniline and polyaniline, ACS Appl. Mater. Interfaces. 6 (2014) 3615–3622. https://doi.org/10.1021/am405868j.

[33] J. Arcot, A. Shrestha, Folate: Methods of analysis, Trends Food Sci. Technol. 16 (2005) 253–266. https://doi.org/10.1016/j.tifs.2005.03.013.

[34] Z. Shi, J. Lipkowski, Chloride adsorption at the Au(111) electrode surface, J. Electroanal. Chem. 403 (1996) 225–239. https://doi.org/10.1016/0022-0728(95)04313-6.

[35] W. Wu, H. Niu, D. Yang, S. Bin Wang, J. Wang, J. Lin, C. Hu, Controlled layer-by-layer deposition of carbon nanotubes on electrodes for microbial fuel cells, Energies. 12 (2019) 1–16. https://doi.org/10.3390/en12030363.

[36] W.S. Alencar, F.N. Crespilho, M.V.A. Martins, V. Zucolotto, O.N. Oliveira, W.C. Silva, Synergistic interaction between gold nanoparticles and nickel phthalocyanine in layer-by-layer (LbL) films : evidence of constitutional dynamic chemistry (CDC), Phys. Chem. Chem. Phys. 11 (2009) 5086–5091. https://doi.org/10.1039/b821915j.

[37] J. Liu, Y. Qin, D. Li, T. Wang, Y. Liu, J. Wang, E. Wang, Highly sensitive and selective detection of cancer cell with a label-free electrochemical cytosensor, Biosens. Bioelectron. 41 (2013) 436–441. https://doi.org/10.1016/j.bios.2012.09.002.

[38] J.J. Castillo, W.E. Svendsen, N. Rozlosnik, P. Escobar, F. Martínez, J. Castillo-León, Detection of cancer cells using a peptide nanotube-folic acid modified graphene electrode, Analyst. 138 (2013) 1026–1031. https://doi.org/10.1039/c2an36121c.

[39] G. Wang, X. He, L. Wang, X. Zhang, A folate receptor electrochemical sensor based on terminal protection and supersandwich DNAzyme amplification, Biosens. Bioelectron. 42 (2013) 337–341. https://doi.org/10.1016/j.bios.2012.10.066.

[40] H.B. Wang, H.D. Zhang, S.P. Xu, T. Gan, K.J. Huang, Y.M. Liu, A sensitive and label-free electrochemical impedance biosensor for protein detection based on terminal protection of small molecule-linked DNA, Sensors Actuators, B Chem. 194 (2014) 478–483. https://doi.org/10.1016/j.snb.2014.01.002.

[41] T. Tian, L. Li, Y. Zhang, H. Liu, L. Zhang, M. Yan, J. Yu, Dual-mode fluorescence biosensor platform based on T-shaped duplex structure for detection of microRNA and folate receptor, Sensors Actuators, B Chem. 261 (2018) 44–50. https://doi.org/10.1016/j.snb.2018.01.129.

***For all figures the color should be used**

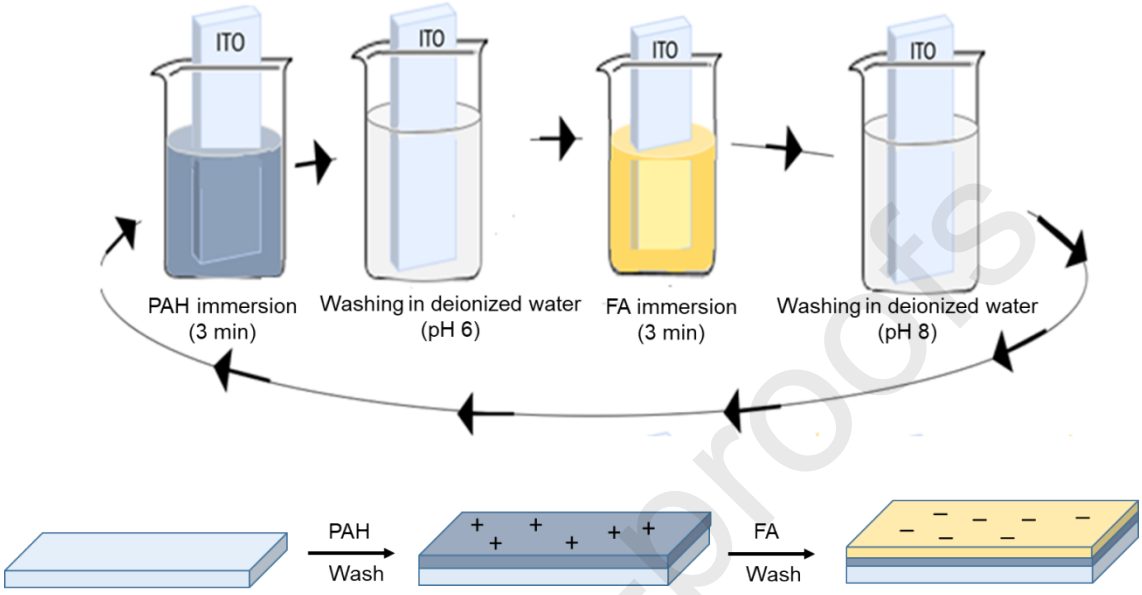

Fig. 1. Schematic representation of [PAH/FA] multilayers assembling by the LbL technique onto ITO substrates

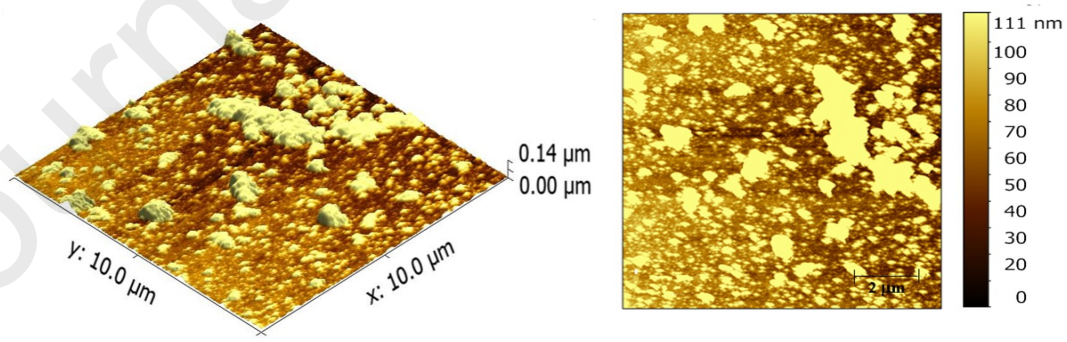

Fig 2. AFM images in 2D (left) and 3D (right) of the $[PAH/FA]_{20}$ film assembled on Si/SiO_2 substrate.

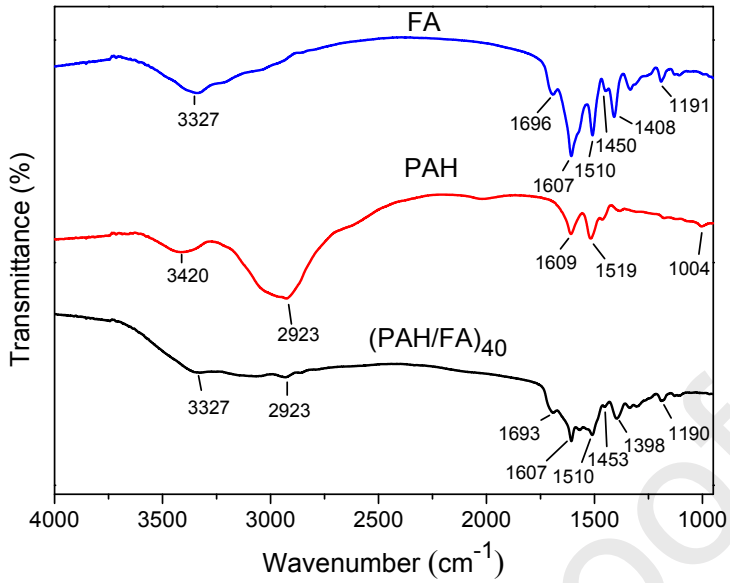

Fig 3. FTIR transmission spectra of FA, PAH and $[PAH/FA]_{40}$ LbL film assembled on Si/SiO_2 substrate.

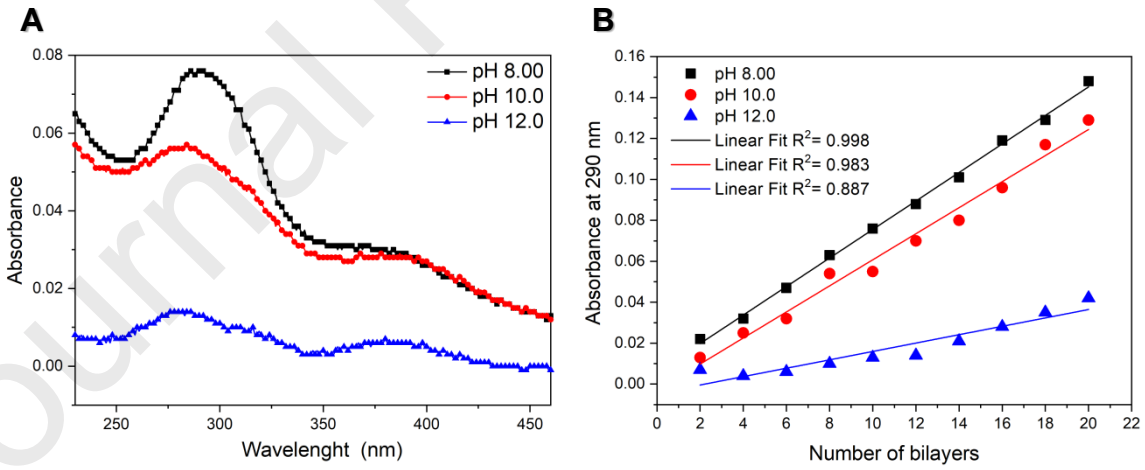

Fig 4. UV–vis absorption spectra (A) and absorbance at 290 nm (B) of $[PAH/FA]_{10}$ films at pHs 8.00, 10.0 and 12.0 assembled on quartz substrate.

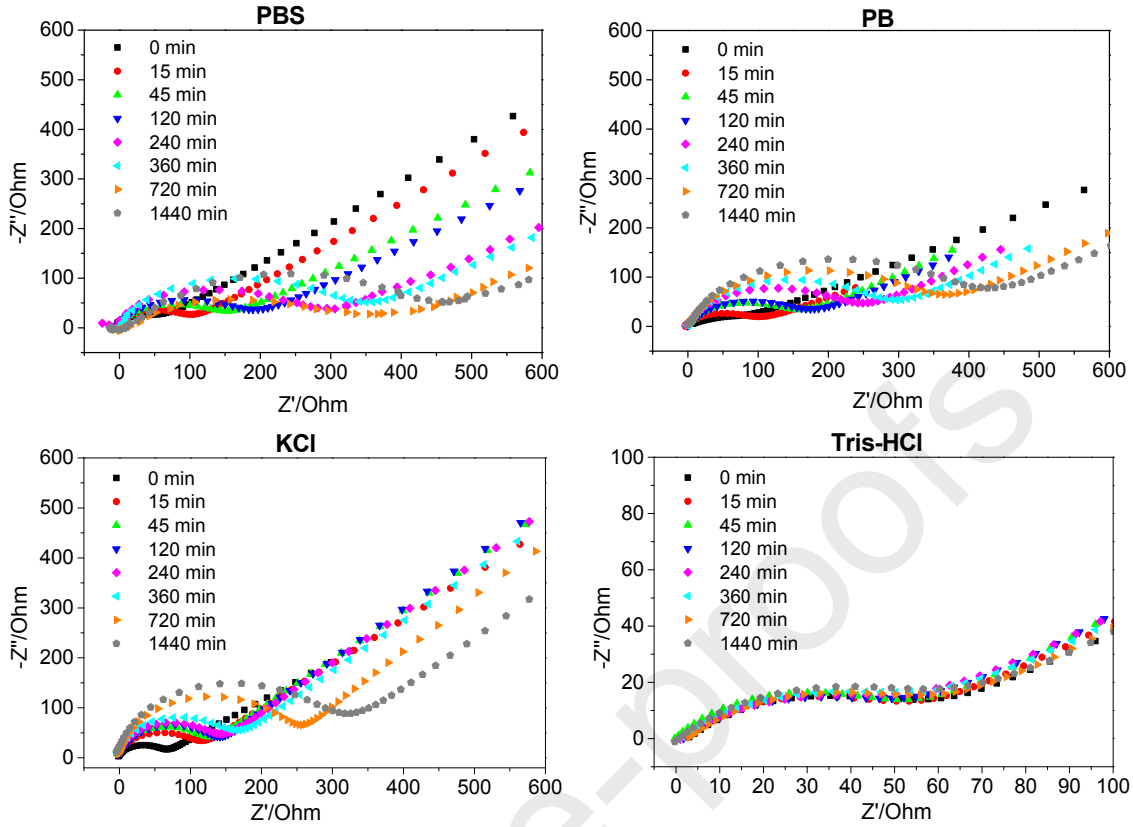

Fig 5. Nyquist plots of $[PAH/FA]_3$ films stored in PBS, PB, KCl and Tris-HCl buffers for up to 1440 min.

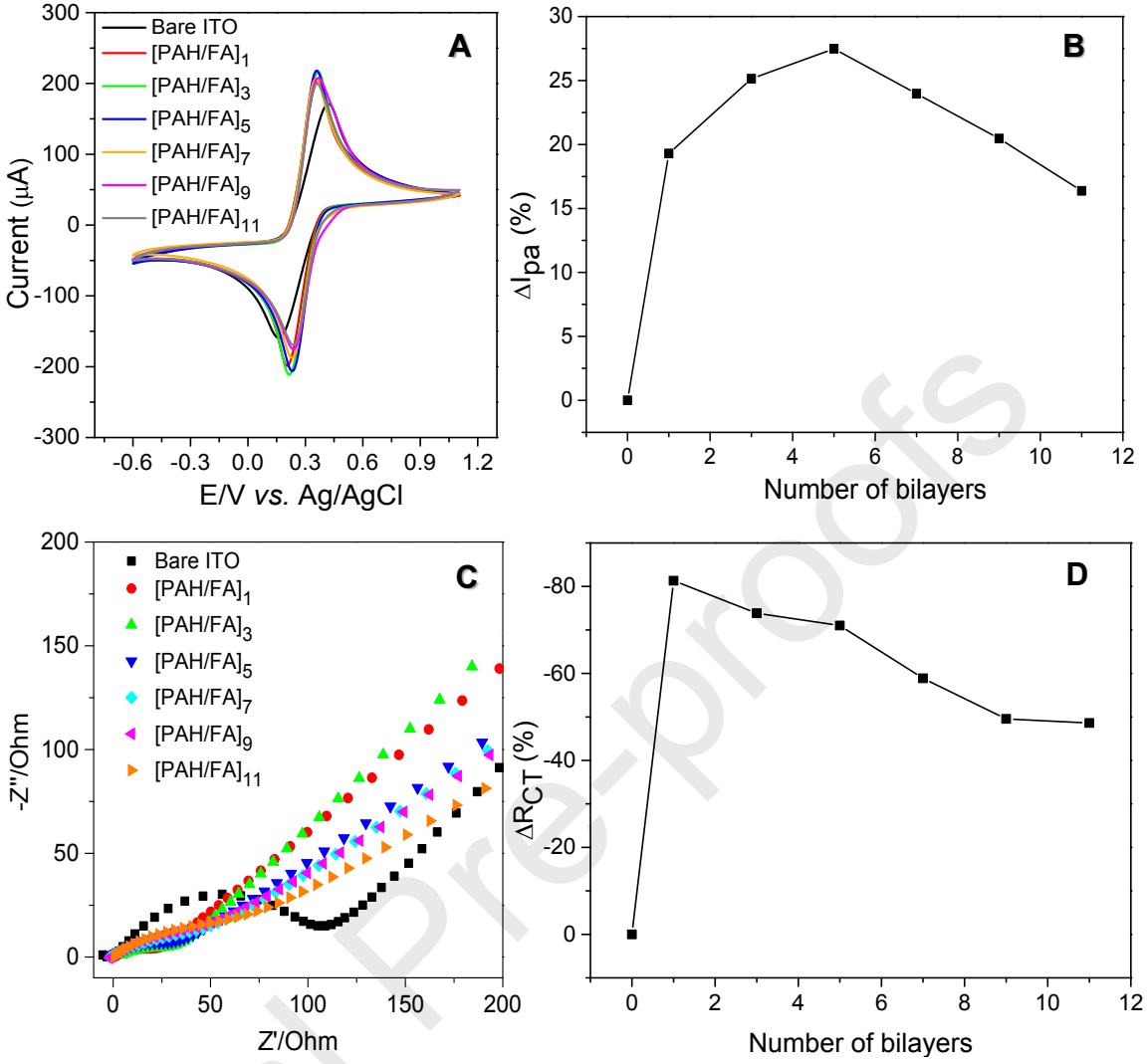

Fig 6. (A) Cyclic voltammograms of the bare ITO and ITO modified with 1, 3, 5, 7, 9 or 11 [PAH/FA] bilayers. (B) Dependence of the normalized anodic current I_{pa} ($\Delta I_{pa} = (I_{pa\ modified\ ITO} - I_{pa\ bare\ ITO}) / I_{pa\ bare\ ITO}$) on bilayer number. (C) Nyquist plots of the bare ITO and ITO modified with 1, 3, 5, 7, 9 or 11 [PAH/FA] bilayers. (D) Dependence of the normalized charge transfer resistance R_{CT} ($\Delta R_{CT} = (R_{CT\ modified\ ITO} - R_{CT\ bare\ ITO}) / R_{CT\ bare\ ITO}$) on bilayer number.

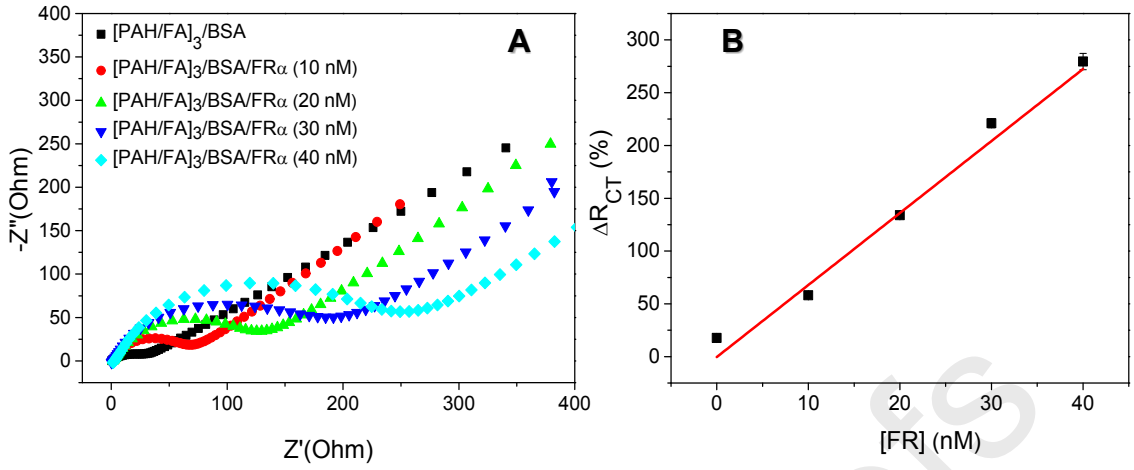

Fig 7. (A) The impedance response of the LBL biosensor towards FRα concentration in the range 10-40 nM. (B) Analytical curve of normalized R_{CT} change against FRα concentration measured in three independent electrodes (n=3) showing a linear relationship.

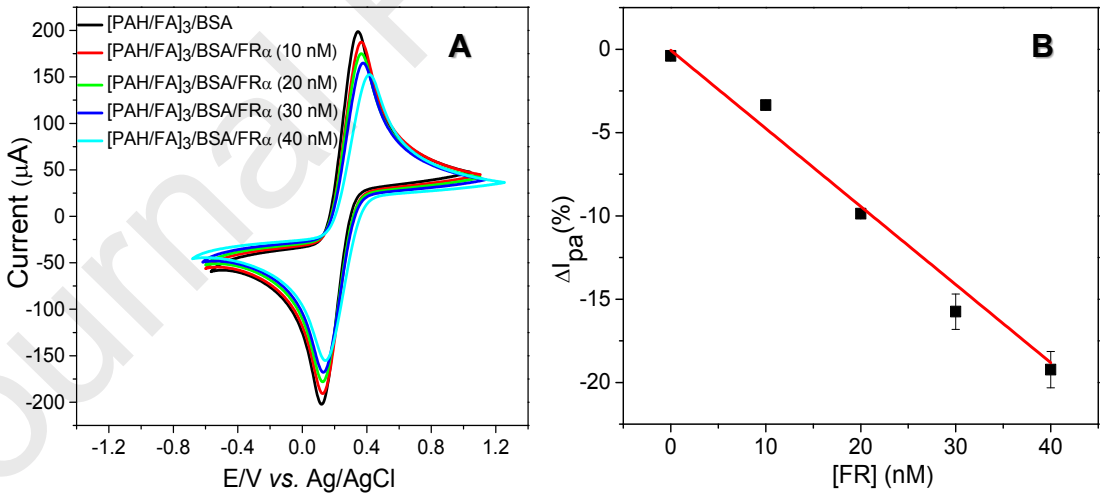

Fig 8. (A) The anodic current of the LBL biosensor as a function of FR-α concentration in the range 10-40 nM. (B) Analytical curve of normalized I_{pa} change against FR-α concentration measured in three independent electrodes (n=3) showing an inversely proportional relationship.

Graphical abstract

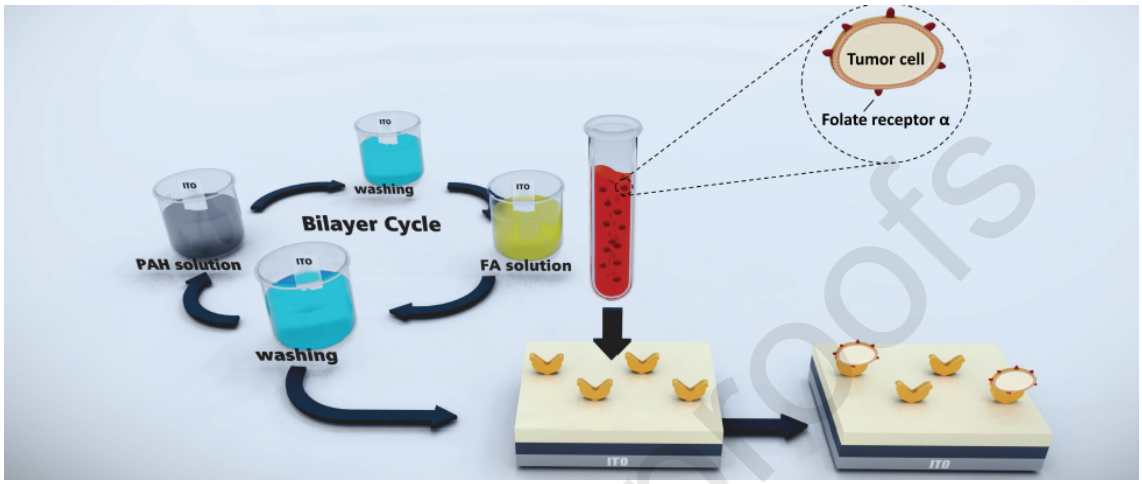

Highlights

- A simple and low-cost electrochemical biosensor based on LBL technique was developed for folate receptors detection.

- Layer-by-layer films were constructed on ITO electrodes by the alternately assembling of polyallylamine hydrochloride and folic acid.

- The biosensor exhibited a linear response to the concentration of the folate receptors

- Good selectivity, reproducibility (RSD of 1.12%), and stability (RSD 6.7%) were achieved

Declaration of interests

☒ The authors declare that they have no known competing financial interests or personal relationships that could have appeared to influence the work reported in this paper.

☐The authors declare the following financial interests/personal relationships which may be considered as potential competing interests: